Anal. Bioanal. Electrochem., Vol. 17, No. 3, 2025, 229-241
https://www.doi.org/10.22034/abec.2025.722375

Analytical & Bioanalytical Electrochemistry

Full Paper

Electrochemical Sensor based on Modified Graphene Paste Electrode Decorated Anatase TiO_2 for Determination of Profenofos Insecticides

Bromo Kusumo Achmad,[1,*] Muhammad Nurdin,[2] Andi Khaeruni,[3] Ramadhan Tosepu,[4] Gusti Ayu Kade Sutariati,[5] Nur Santy Asminaya,[6] Malidiyah Malidiyah,[2] Sartiah Yusran,[7] and Nohong, Nohong[2]

[1]*Doctoral student of Agricultural Sciences, Universitas Halu Oleo, Kendari 93121 – Southeast Sulawesi, Indonesia*
[2]*Department of Chemistry, Faculty of Mathematics and Natural Sciences, Universitas Halu Oleo, Kendari 93232-Southeast Sulawesi, Indonesia*
[3]*Department of Plant Protection, Faculty of Agriculture, Universitas Halu Oleo, Kendari 93232–Southeast Sulawesi, Indonesia*
[4]*Deparment of Health Administration, Faculty of Public Health, Universitas Halu Oleo, Kendari 93232–Southeast Sulawesi, Indonesia*
[5]*Department of Agrotechnology, Faculty of Agriculture, Universitas Halu Oleo, Kendari 93232–Southeast Sulawesi, Indonesia*
[6]*Faculty of Animal Science, Universitas Halu Oleo, Kendari 93232–Southeast Sulawesi, Indonesia*
[7]*Faculty of Public Health, Universitas Halu Oleo, Kendari 93232–Southeast Sulawesi, Indonesia*

*Corresponding Author, Tel.: +82221717148
E-Mail: bromo.ka@gmail.com

Received: 3 February 2025 / Received in revised form: 23 March 2025 / Accepted: 29 March 2025 / Published online: 31 March 2025

Abstract- Profenofos (PFF) is a highly toxic organophosphate insecticide, necessitating the development of rapid and sensitive detection methods. In this study, we developed an electrochemical sensor based on anatase TiO_2-modified graphene (G/TiO_2 anatase) for the efficient detection of PFF. Characterization using SEM, XRD, and FTIR confirmed the successful formation of anatase-phase TiO_2 nanoparticles on graphene sheets. Electrochemical performance evaluation via cyclic voltammetry demonstrated that the G/TiO_2 anatase electrode exhibited superior redox behavior compared to bare graphene and TiO_2 nanoparticles. The sensor achieved a low limit of detection (LOD) of 0.046 µg/L and a limit of quantification (LOQ) of 0.153 µg/L, within a linear detection range of 0.1–0.9 µg/L. Additionally, it showed

excellent repeatability, with a relative standard deviation (%RSD) of 2.48%. These findings highlight the potential of G/TiO_2 anatase as a highly sensitive and reliable electrochemical sensor for PFF detection. The proposed sensor provides a rapid, simple, and efficient alternative for direct PFF analysis, which could be beneficial for environmental monitoring and food safety applications.

Keywords- Anatase TiO_2; Graphene; Profenofos; Electrochemical sensor; Cyclic voltammetry

1. INTRODUCTION

Currently, organophosphate insecticides, such as profenofos (PFF), are widely used as dominant agents to control pests and insects on crops. Their extensive application is attributed to their high effectiveness in protecting crops from damage caused by pest organisms [1,2]. Despite their efficacy, the presence of pesticide residues in agricultural products has become a major concern due to its potential impact on human health and the environment. According to the World Health Organization (WHO), PFF is classified as a Class II toxic substance, as it is considered highly hazardous to humans [3–5]. Exposure to PFF may result in serious health issues, including neurological and respiratory disorders, and can even lead to death if not managed properly [6,7]. Moreover, environmental contamination from profenofos residues poses risks, particularly when these residues pollute water sources and soil, thereby affecting the human food chain. Consequently, there is an ongoing need for the development of rapid, sensitive, and cost-effective methods for detecting PFF residues in agricultural products.

Several common methods have been applied to detect profenofos insecticide residues, such as GC-MS [8], HPLC [9], spectrophotometry [10], fluorescence [11], electrophoresis [12], and enzyme immunoassay [13]. Although these techniques are highly sensitive, they present challenges related to high costs, lengthy analysis times, complex laboratory equipment, and limited applicability. Furthermore, these methods often require skilled experts for operation. Consequently, the development of alternative methods that are simpler, cost-effective, rapid, and sensitive for detecting profenofos insecticides remains an important topic [14]. Electrochemical methods have been regarded as highly sensitive, portable, and effective approaches for analyzing various critical molecules, including active ingredients in pharmaceutical products, aqueous solutions, and even human body fluids.

The development of electrochemical sensors has increasingly focused on modifying working electrode materials using metal nanomaterials. To the best of our knowledge, various working electrodes have been reported and applied for the detection of profenofos using voltammetric techniques. For example, Azis et al. [15] reported an electrochemical sensor based on a carbon paste electrode (CPE) modified with TiO_2 nanoparticles. Parab et al. [16] have modified a non-enzymatic sensor based on a glassy carbon electrode (GCE) with ZnO nanoparticles for the rapid detection of trace paraoxon in water and food samples. Shi et al. [17] also explain the ultrasensitive analysis of profenofos residue based on MWCNTs modified with Au@AgNPs nanoparticles. Although various working electrode materials have been

developed and applied for the detection of profenofos (PFF) using electrochemical techniques, these electrodes still possess certain intrinsic limitations, such as relatively low detection sensitivity, and poor chemical and thermal stability. In this study, we investigate the characteristics of graphene as a working electrode material for detecting the insecticide profenofos.

Recently, there has been significant interest in the application of nanomaterials as modification agents in electrochemical sensors. Titanium dioxide (TiO_2) nanoparticles, particularly in the anatase phase, have become one of the most widely used metal oxides for electrode modification due to their outstanding properties [18,19]. With its unique crystal structure, anatase TiO_2 exhibits excellent chemical stability, is non-toxic, and is environmentally friendly [20,21]. Moreover, anatase TiO_2 is highly appealing for sensor applications due to its high mechanical rigidity, large surface area, and high pore volume, which can enhance electrode performance [22–24]. The superior electronic properties of anatase TiO_2 highlight its capability to improve electron transfer processes and provide optimal electrocatalytic performance, making it a promising candidate for working electrode modification.

In this work, we designed G/TiO_2 anatase as a working electrode for the electrochemical detection of the insecticide profenofos. Initially, the G/TiO_2 anatase electrode was tested in a $[Fe(CN)_6]^{3-/4-}$ solution as a redox probe. The prepared nanocomposite was characterized by SEM, XRD, and FTIR spectroscopy. Under optimal experimental conditions, the electrochemical sensor for PFF detection exhibited good sensitivity and stability. Furthermore, measurement parameters such as scan rate, detection limit, reproducibility, stability, and real sample testing were investigated and optimized. This study provides a promising approach for developing reliable electrochemical sensors for pesticide monitoring in environmental and food safety applications.

2. EXPERIMENTAL SECTION

2.1. Apparatus

Cyclic voltammetry (CV) was performed using an Autolab DY2000 electrochemical system connected to a computer. The CV test was analyzed under optimized instrument settings as follows: a scan rate of 10 $mV.s^{-1}$ and a potential window of -0.8 to 0.8 V. In this electrochemical experiment, a three-electrode system was employed, where the G/TiO_2 anatase electrode served as the working electrode, the Ag/AgCl electrode acted as the reference electrode, and a Pt wire was used as the counter electrode. Additionally, FTIR analysis was conducted to identify the functional groups present in the electrode material. XRD was utilized to confirm the crystal structure and phase of the sample, while SEM was performed to examine the morphology of the synthesized sample.

2.2. Reagents and Chemicals

Profenofos and graphene powder were acquired from Sigma Aldrich, China. A stock solution of profenofos (100 ppm) was prepared using ethanol as the solvent. Sodium nitrate was obtained from New Praktika Alkesindo, and a 0.01 M solution was prepared in water as the solvent. This solution was utilized as a supporting electrolyte in the measurements. Anatase TiO_2 powder was prepared according to the methodology outlined by Nurdin et al. (2024). In brief, two solutions (A and B) were prepared via the sol-gel technique as follows. Solution A, containing 4.0 mL of titanium tetraisopropoxide (TTIP), was dissolved in 15.0 mL of ethanol and 0.5 mL of acetylacetone. Solution B was composed of 15.0 mL of ethanol, 2.0 mL of distilled water, and 1.0 mL of acetic acid. Subsequently, the two solutions were mixed and refluxed for 3 hours at a temperature of 50 °C while being vigorously stirred. The liquid was then left overnight at room temperature to form a gel. The final step involved calcining the sample at 500 °C for 3 hours.

2.3. Preparation of working electrode

The G/TiO_2 anatase electrode was prepared by mixing graphene powder, paraffin oil, and TiO_2 anatase nanoparticles in a weight ratio of 7:3 (w/w). All components were blended using a mortar and pestle to obtain a homogeneous G/TiO_2 anatase paste. The unmodified electrode (graphene) was prepared by mixing graphene powder and paraffin oil in the same weight ratio of 7:3 (w/w). The ratio of graphene powder to paraffin oil remained consistent for all electrodes. Subsequently, the obtained G/TiO_2 anatase paste (G/TiO_2 anatase) was placed into an electrode body with a diameter of 3 mm that had been pre-prepared. The surface of the electrode was smoothed by polishing it on sandpaper before use. Copper wire was utilized as an electrical connector by inserting it through the open end of the electrode body filled with the G/TiO_2 anatase paste.

2.4. Electrochemical measurements

All electrochemical measurements were conducted using an Autolab DY2000 potentiostat with a conventional three-compartment setup. The working electrode employed was G/TiO_2 anatase, while Ag/AgCl served as the reference electrode, and a Pt wire served as the counter electrode. The electrochemical response of PFF was measured using G/TiO_2 anatase. A standard solution of PFF was added to the electrochemical cell containing 20 mL of a supporting electrolyte solution of 0.01 M $NaNO_3$ and a citrate buffer at pH 4. Cyclic voltammetry (CV) measurements were performed over a potential range of -0.8 V to 0.8 V, with a scan rate of 10 mV/s and a time duration of 1 second. Measurements using cyclic voltammetry (CV) were conducted at a scan rate of 10 mV/s throughout a potential range of -0.8 V to 0.8 V.

3. RESULTS AND DISCUSSION

3.1. Structural, morphological, and chemical characterization of G/TiO_2 anatase composites

3.1.1. X-ray Diffraction (XRD) analysis

XRD analysis was conducted to investigate the structure and crystal phases of pure graphene, TiO_2 nanoparticles, and G/TiO_2 anatase composites. The X-ray diffraction patterns of the graphene nanocomposite, TiO_2 nanoparticles, and G/TiO_2 anatase are shown in Figure 1. The XRD pattern of graphene (Figure 1a) displays a prominent peak at 2θ = 19.09°, corresponding to the (002) plane. This peak indicates a characteristic interlayer spacing in the graphene structure, suggesting a high degree of crystallinity [25]. As is well-known, pure graphene typically exhibits a peak around 2θ = 26°, associated with well-ordered graphite layers. However, the observed shift in our study may be attributed to variations in interlayer spacing, possibly caused by residual oxygen-containing functional groups or slight structural defects that occurred. Significant diffraction peaks at 25.3°, 37.8°, 48.0°, 53.9°, 55.1°, and 62.7° are also visible in the XRD pattern of TiO_2 nanoparticles (Figure 1b) which are characteristics of TiO_2 in the anatase phase (JCPDS card no. 21-1272) [26,27]. This phase is well-known for its high photocatalytic activity and stability [28]. In the XRD spectrum of the G/TiO_2 composite (Figure 1c), the prominent anatase peaks of TiO_2 are retained, indicating that the composite maintains the anatase phase. The (002) peak of graphene is also present but with reduced intensity, suggesting partial coverage of the graphene sheets by TiO_2 nanoparticles. The integration of TiO_2 into the graphene sheets may enhance electron mobility and facilitate effective electron transfer, which is beneficial for electrochemical sensing applications [29].

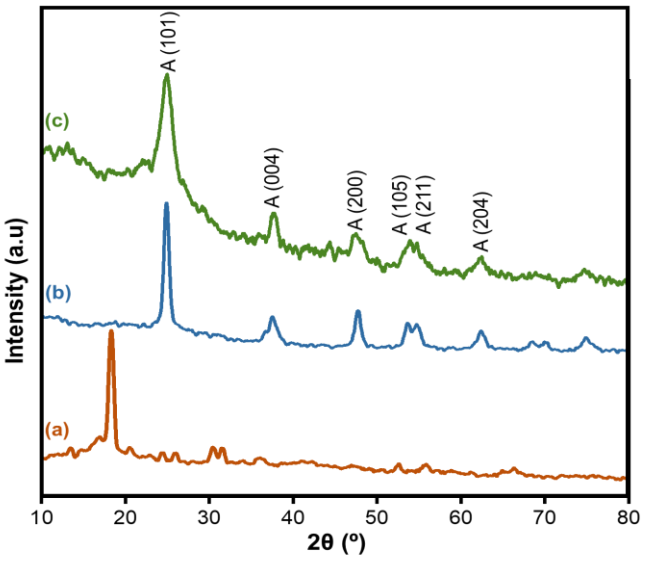

Figure 1. XRD spectra of graphene (a), TiO_2 NPs (b), and G/TiO_2 anatase (c)

3.1.2. FTIR analysis

FTIR spectroscopy is employed to analyze chemical bonds and functional groups in graphene, TiO_2 nanoparticles, and G/TiO_2 anatase composites. The FTIR spectra for all samples are presented in Figure 2. The broad absorption bands observed for all samples correspond to the O-H stretching mode, indicating the presence of hydroxyl groups (at 3470 cm^{-1} and 1680 cm^{-1}). Meanwhile, specific peaks around 480 cm^{-1} and 660 cm^{-1} correspond to Ti–O and Ti–O–Ti stretching vibrations, characteristic of anatase-phase TiO_2 [30,31] . In the G/TiO_2 composite spectrum, these peaks are retained, confirming the structural integrity of TiO_2 in the composite. Additionally, the G/TiO_2 composite shows a peak around 1630 cm^{-1}, corresponding to C=C stretching, which is characteristic of the graphene structure. This confirms the successful bonding between graphene and TiO_2, which may enhance sensor conductivity and sensitivity due to the synergistic effect between these materials.

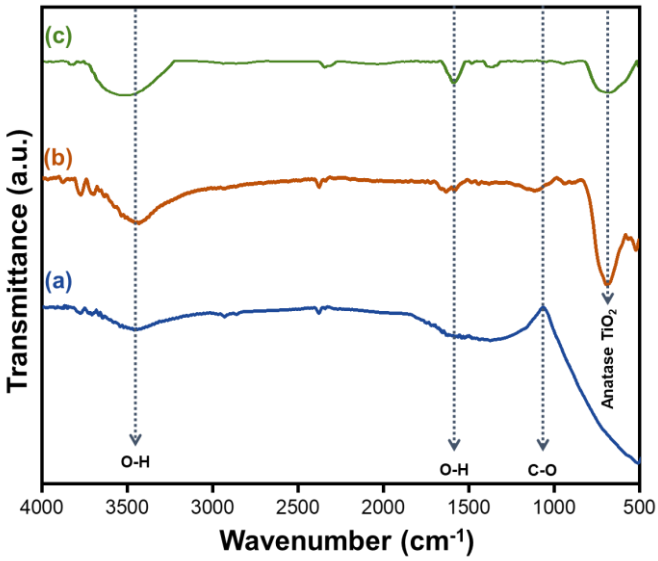

Figure 2. FTIR spectra of graphene (a), TiO_2 NPs (b), and G/TiO_2 anatase (c)

3.1.3. SEM analysis

The morphology and surface characteristics of graphene, TiO_2 nanoparticles, and G/TiO_2 anatase composites were analyzed using Scanning Electron Microscopy (SEM). The SEM images provide insights into the structure and distribution of TiO_2 nanoparticles on the graphene surface, which is crucial for understanding the electrochemical properties of the composite. As seen in Figure 3a, pure graphene exhibits a characteristic sheet-like morphology with a relatively smooth and wrinkled surface. This morphology is typical of graphene, providing a large surface area. Additionally, Figure 3a displays an irregular structure as a result of the graphite particles' separation. Subsequently, Figure 3b shows well-dispersed, round particles consistent with the anatase phase. The relatively small particle size and high surface area of TiO_2 are essential for enhancing the catalytic properties of the composite [32,33]. This

feature provides numerous active sites, which is beneficial for the electrochemical performance of the sensor. Meanwhile, the G/TiO_2 anatase composite (Figure 3c) shows a uniform distribution of TiO_2 nanoparticles over the graphene sheets, indicating the successful integration of TiO_2 into the graphene matrix. This distribution is expected to enhance electron transfer between TiO_2 and graphene, thereby increasing sensitivity in profenofos electrochemical sensing. Additionally, the images reveal that the TiO_2 particles are tightly attached to the graphene surface, indicating strong interfacial interaction.

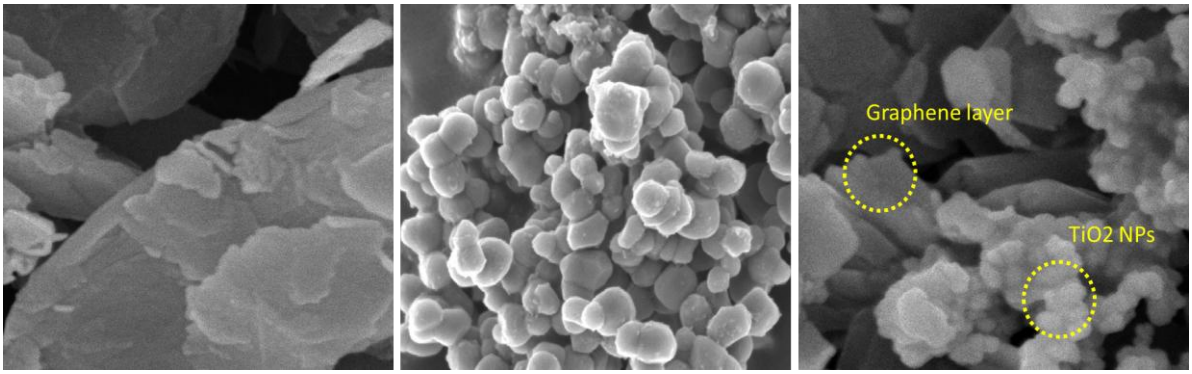

Figure 3. SEM images of graphene (a), TiO_2 NPs (b), and G/TiO_2 anatase (c)

3.2. Electrochemical behavior of G/TiO_2 in K_3FeCN_6 solution

All electrodes were electrochemically characterized using cyclic voltammetry in 0.01 M K_3FeCN_6 over a potential range of -0.8 V to 0.8 V (Figure 4). On bare graphene (curve a), a pair of distinct redox peaks characteristic of the $[Fe(CN)_6]^{3-/4-}$ couple was clearly observed [34,35] In contrast, for the TiO_2 NP electrode (curve b), no clear redox peak currents were detected, indicating limited redox activity. The peak currents for the graphene and TiO_2 NP electrodes were 1.36 µA and 3.18 µA, respectively. When the graphene electrode was modified with TiO_2 nanoparticles (curve c), a notable increase in redox peak current was observed (I_{pa} = 4.83 µA, I_{pc} = -6.01 µA), along with a positive shift in potential. This phenomenon can be attributed to the superior catalytic activity of TiO_2 nanoparticles in facilitating electron transport.

Table 1. Electrochemical characterization of G/TiO_2 anatase electrode, TiO_2 NPs, and graphene

Electrode	I_{pa} (µA)	I_{pc} (µA)	E_{pa} (V)	E_{pc} (V)
G/TiO_2 anatase	4.83	-6.01	0.08	-0.26
TiO_2 NPs	3.18	-3.71	0.07	-0.29
Graphene	1.36	-2.36	0.02	-0.31

Additionally, the synergistic effect and substantial surface area contribute significantly to enhancing the conductivity of the G/TiO_2 anatase electrode, enabling more efficient current conduction to the electrode surface. Table 1 lists the anodic (I_{pa}) and cathodic (I_{pc}) currents of the G/TiO_2 anatase, TiO_2 NP, and graphene electrodes.

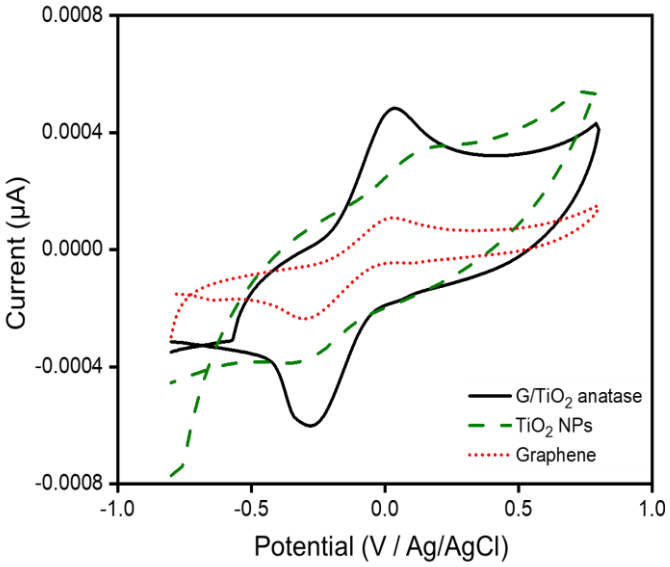

Figure 4. Cyclic voltammograms in 0.01 M K_3FeCN_6 containing 0.1 M $NaNO_3$ for (a) G/TiO_2 anatase (b) TiO_2 NPs (c) bare graphene

3.3. Electrochemical sensing of profenofos

To determine the response of the G/TiO_2 anatase electrode to profenofos solution, a study was conducted on the effect of scan rate. The scan rate is an essential factor in electrochemical studies as it influences the adsorption rate of species on the electrode surface [36].

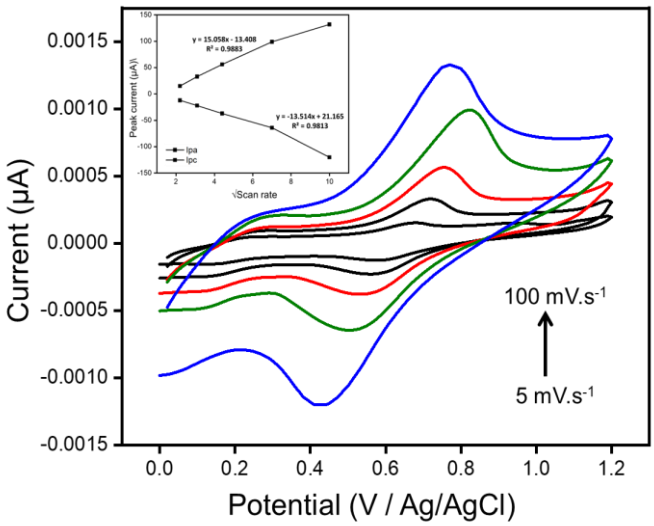

Figure 5. Scan rate analysis of PFF redox based on G/TiO_2 anatase and (B) Square root of scan rates with calibration plot

The effect of scan rate on the voltammogram of profenofos at the G/TiO_2 anatase electrode was investigated in a citrate buffer solution (PBS) at pH 4 (Figure 5). It was observed that the plot of anodic peak current (I_{pa}) and cathodic peak current (I_{pc}) displayed a linear relationship with scan rates (5 mV.s^{-1} – 100 mV.s^{-1}). The linear relationship between the peak current and the square root of the scan rate indicates that the redox process of profenofos is controlled by diffusion current (Figure 5). Furthermore, the plot of anodic peak current (I_{pa}) and cathodic peak current (I_{pc}) versus scan rate exhibited a good correlation coefficient (0.9883 and 0.9813).

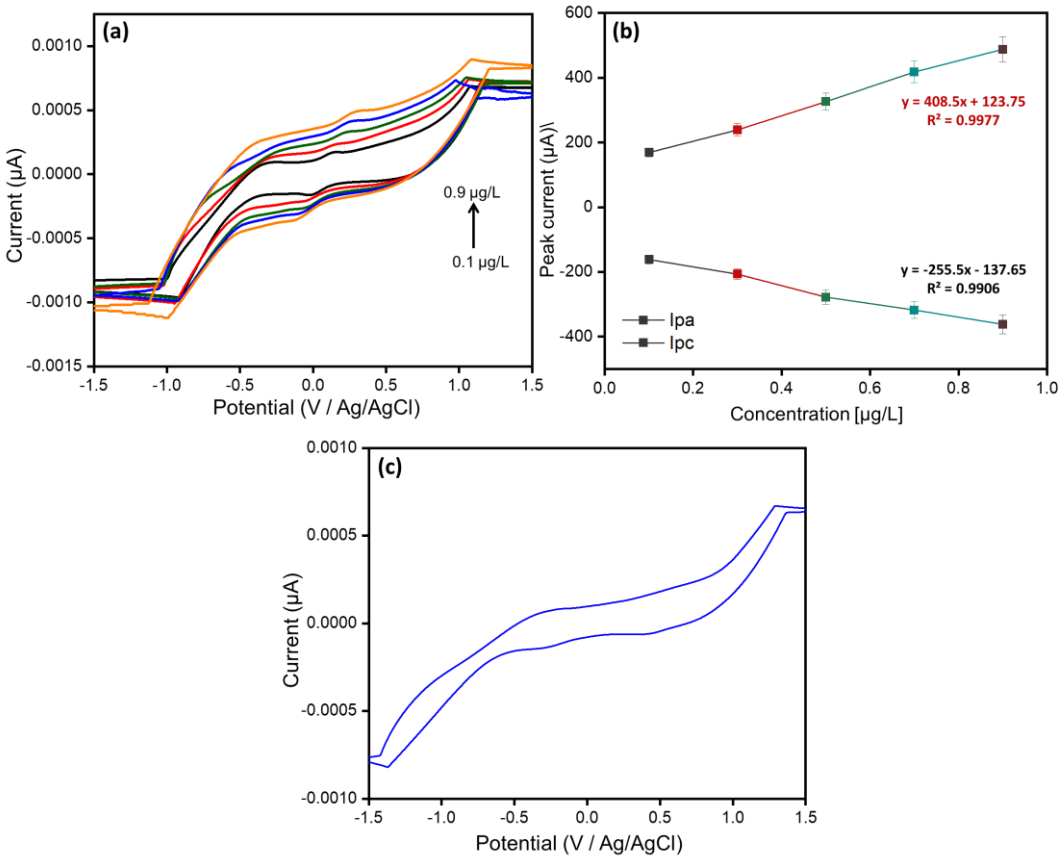

Figure 6. (a) CV at different of PFF concentrations at scan rate 100 mV.s^{-1} and (c) Cyclic voltammogram of citrate buffer pH 4

The electrochemical determination of PFF using G/TiO_2 anatase modified electrodes was conducted via CV. Figure 6a illustrates the response of the G/TiO_2 anatase electrode to various concentrations of PFF ranging from 0.1 to 0.9 µg/L. It is clear that the produced redox current rises in tandem with the PFF concentration. This phenomenon can be attributed to the surface interaction between PFF and the active material of the electrode, resulting in a more efficient electron transfer process on the modified electrode surface [19,37]. Furthermore, the inset of Figure 6a presents the calibration curve analysis, which indicates a linear relationship between the peak redox currents (I_{pa} and I_{pc}) and the concentration of PFF. The linear regression equations are given as I_{pa}: y = 408.5x + 123.75 and I_{pc}: y = -255.5x - 137.65, with correlation

coefficients R^2 = 0.9977 and R^2 = 0.9906, respectively. These R^2 values, which approach 1, indicate the accuracy and precision of the developed sensor in detecting PFF at low concentrations. Additionally, the sensitivity of the G/TiO_2 electrode towards PFF may be attributed to the anatase modification of TiO_2, which enhances the active surface area and accelerates electron transfer. The anatase structure of TiO_2 is known to possess electronic properties that support better redox processes. The limits of detection (LOD) and quantification (LOQ) were then calculated using the formulas LOD = 3SD/m and LOQ = 10SD/m, where m is the calibration curve's slope and SD is the blank samples' standard deviation. (Table 2). The resulting LOD and LOQ values were 0.046 µg/L and 0.153 µg/L, respectively, for the G/TiO_2 anatase electrode.

Table 2. Calibration plot characteristics of PFF were examined using the CV technique

Characteristic	**G/TiO_2 anatase**
Linearity range (µ/L)	0.1 – 0.9
Slope	408.5
Intercept	123.75
Correlation coefficient (R^2)	0.9977
Slope RSD (%)	1.53
Intercept RSD (%)	5.06
Number of data points	5
Standard deviation (SD)	6.27
LOD (µ/L)	0.046
LOQ (µ/L)	0.153

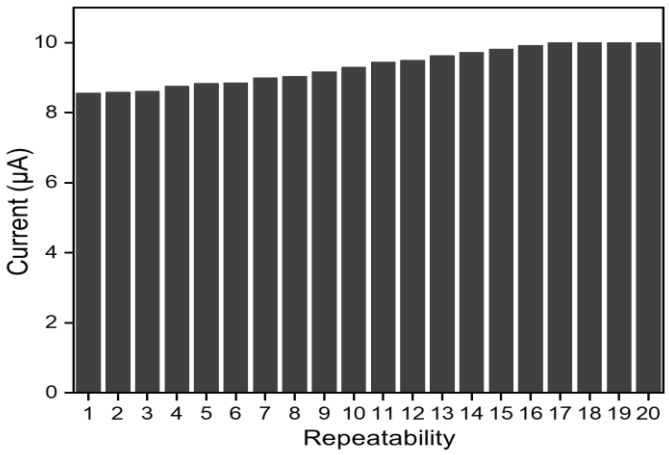

Figure 7. The repeatability of G/TiO_2 anatase electrode with 20 replications

Furthermore, this study also conducted a repeatability test of the electrode. The repeatability test is an important parameter in evaluating the performance of the electrode, as it reflects the electrode's ability to provide consistent measurement results when used

repeatedly under the same conditions [19,38]. The repeatability of the G/TiO_2 anatase electrode was investigated in a PFF solution at a concentration of 0.1 µg/L over 20 repetitions (Figure 7). The measurement results indicated that the obtained % RSD value was 2.68%.

Table 3. Comparison of different working electrode materials for detecting pesticides with current research

Electrode material	Electrochemical techniques used	Analyte	Sensitivity	Reference
MWCNTs/TiO_2NPs	CV, DPV	Diazinon	11–8360 nM	[39]
GCE/ZnOHS	CV, DPV	Parathion	0.5×10^{-9} mol L^{-1}	[40]
TiO_2/CPE	CV, SWV	Carbendazim	1.71×10^{-8} M	[41]
Activated carbon/TiO_2	SWV	Dichlorophen	1.01×10^{-8} M	[42]
G/TiO_2 anatase	**CV**	**Profenofos**	**0.046 µ/L**	**This work**

4. CONCLUSION

In this study, an electrochemical sensor for detecting PFF based on graphene-incorporated anatase TiO_2 has been successfully developed. The G/TiO_2 anatase electrode was effectively prepared using a simple sol-gel method. The characteristics and electrochemical behavior of the G/TiO_2 anatase have also been successfully reported. It was found that the G/TiO_2 anatase electrode exhibited superior electrochemical performance compared to other investigated electrodes (Table 3). This phenomenon indicates that electrochemical activity can be enhanced by controlling the crystallinity and particle size distribution of the graphene electrode. The developed G/TiO_2 anatase electrode demonstrated a good detection response with a linear range of 0.1–0.9 µg/L, a detection limit of 0.046 µg/L, and a limit of quantification of 0.153 µg/L. Additionally, the electrode showed good stability and reproducibility, indicating its significant potential for the determination of PFF compounds in agricultural samples.

Acknowledgments

This study was financially supported by the Yayasan Mandala Waluya Kendari. Furthermore, we acknowledge the support of the IndoLab Group and laboratory facilities.

Declarations of interest

The authors declare no conflict of interest in this reported work.

REFERENCES

[1] M.U. Ghani, H.N. Asghar, A. Niaz, Z.Z. Ahmad, M.F. Nawaz, and M.M. Häggblom, Int. J. Phytoremediation 24 (2022) 463.

[2] R. Bibi, M. Ahmad, A. Gulzar, and M. Tariq, Int. J. Trop. Insect. Sci. 42 (2022) 379.
[3] O.A. Dadson, C.A Ellison, S.T. Singleton, L.H. Chi, B.P. McGarrigle, P.J. Lein, F.M. Farahat, T. Farahat, and J.R. Olson, Toxicology 306 (2013).
[4] M. Kushwaha, S. Verma, and S. Chatterjee, J. Environ. Qual. 45 (2016) 1478.
[5] L. Ding, J. Wei, Y. Qiu, Y. Wang, Z. Wen, J. Qian, N. Hao, C. Ding, Y. Li, and K. Wang, Chem. Eng. J. 407 (2021) 127213.
[6] B. Maddah, A. Sabouri, and M. Hasanzadeh, J. Polym. Environ. 25 (2017) 770.
[7] A. Raj, A. Kumar, and P.K. Khare, Environ. Sci. Pollut. Res. 31 (2024) 14367.
[8] A.A. Abdalla, A.S. Afify, I.E. Hasaan, and A. Mohamed, Food Anal. Methods 11 (2018) 382.
[9] T.T. Hu, C.M. Lu, H. Li, Z.X. Zhang, Y.H. Zhao, and J. Li, Anal. Sci. 33 (2017) 1027.
[10] Z. Lu, J. Li, J. Shen, and H. Wang, Anal. Lett. 56 (2023) 1514.
[11] F. Liu, S. Zhao, X. Lai, Y. Fan, P. Han, and L. Chen, Food Chem. 393 (2022) 133321.
[12] G. Selvolini, I. Băjan, O. Hosu, C. Cristea, R. Săndulescu, and G. Marrazza, Sensors 18 (2018) 2035.
[13] Y. Yue, J. Chen, M. Zhang,Y. Yin, and Y. Dong, Anal. Lett. 55 (2022) 1701.
[14] M. Nurdin, M.Z. Muzakkar, M. Maulidiyah, C. Sumarni, T. Azis, R. Ratna, M. Natsir, I. Irwan, L.O.A. Salim, and A.A. Umar, J. Appl. Electrochem. 53 (2022) 307.
[15] T. Azis, M. Maulidiyah, M.Z. Muzakkar,R. Ratna, S.W. Aziza, C.M. Bijang, A.O. Prabowo, D. Wibowo, and M. Nurdin, Surf. Eng. Appl. Electrochem. 57 (2021) 387.
[16] A.E. Parab, K. Mohanapriya, and N. Jha, Mater. Today Proc. 42 (2021) 710.
[17] X. Shi, H. Liu, M. Zhang, F. Yang, J. Li, Y. Guo, and X. Sun, Sensors Actuators B Chem. 348 (2021) 130663.
[18] I. Irwan, I.S. Jumbi, A. Alimin, R. Ratna, N. Nohong, M. Maulidiyah, M. Nurdin, and M.Z. Muzakkar, Anal. Bioanal. Electrochem. 15 (2023) 556.
[19] Z. Arham, M. Maulidiyah, G.A.K. Sutariati, L.O.S. Bande, A. Alimin, H. Ritonga, and M. Nurdin, Electrocatalysis 16 (2025) 171.
[20] M. Nurdin, O.A. Prabowo, Z. Arham, D. Wibowo, M. Maulidiyah, S.K.M. Saad, and A.A. Umar, Surfaces and Interfaces 16 (2019) 108.
[21] D. Wibowo, W.O.S Indah, A. Said, F. Mustapa, B. Susianti, M. Maulidiyah, and M. Nurdin, Anal. Bioanal. Electrochem. 14 (2022) 385.
[22] M. Nurdin, A.H. Watoni, M. Natsir, S. Rahmatilah, M. Maulidiyah, D. Wibowo, L.O.A. Salim, S.N. Sadikin,C.M. Bijang, and A.A. Umar, Korean J. Chem. Eng. 40 (2023) 2290.
[23] M. Nurdin, M.Z. Muzakkar, M. Maulidiyah, T. Trisna, A. Arham, L.O.A. Salim, I. Irwan, and A.A. Umar, Electrocatalysis 13 (2022) 580.
[24] M. Nurdin, I. Ilham, M. Maulidiyah, M.Z. Muzakkar, D. Wibowo, Z. Arham,L.O.A. Salim, I. Irwan, C. Bijang, and A.A. Umar, Electrocatalysis 14 (2023) 281.

[25] M. Sharma, S. Rani, D.K. Pathak, R. Bhatia, R. Kumar, and I. Sameera, Carbon 184 (2021) 437.
[26] H.A.R.A. Hussian, M.A.M. Hassan, and I.R. Agool, Optik (Stuttg) 127 (2016) 2996.
[27] K.A. Jacob, P.M. Peter, P.E. Jose, C.J. Balakrishnan, and V.J. Thomas, Mater. Today Proc 49 (2022) 1408.
[28] D. Wibowo, Y. Sufandy, I. Irwan, T. Azis, M. Maulidiyah, and M. Nurdin, J. Mater. Sci. Mater. Electron. 31 (2020) 14375.
[29] M. Nurdin, M. Maulidiyah, M.Z. Muzakkar, and A.A. Umar, Microchem. J. 145 (2019) 756.
[30] M. Natsir, Y.I. Putri, D. Wibowo, M. Maulidiyah, L.O.A. Salim, T. Azis, C.M. Bijang, F. Mustapa, I. Irwan, and Z. Arham, J. Inorg. Organomet. Polym. Mater 131 (2021) 3378.
[31] M. Maulidiyah, T. Azis, L. Lindayani, D. Wibowo, L.O.A. Salim, A. Aladin, and M. Nurdin, J. Electrochem. Sci. Technol 10 (2019) 394.
[32] M. Nurdin, L. Agusu, A.A.M. Putra, M. Maulidiyah, Z. Arham, D. Wibowo, M.Z. Muzakkar, and A.A. Umar, J. Phys. Chem. Solids 131 (2019) 104.
[33] M. Nurdin, Z. Arham, W.O. Irna, M. Maulidiyah, K. Kurniawan, I. Irwan, and A.A. Umar, Mater. Sci. Semicond. Process 151 (2022) 106994.
[34] M. Nurdin, N. Dali, I. Irwan, M. Maulidiyah, Z. Arham, R. Ruslan, B. Hamzah, S. Sarjuna, and D. Wibowo, Anal. Bioanal. Electrochem. 10 (2018) 1538.
[35] K.S. Yunita, I. Irwan, and T. Nakai, Surf. Eng. Appl. Electrochem. 59 (2023) 764.
[36] Z. Arham, and K. Kurniawan, Korean J. Chem. Eng. 39 (2022) 1333.
[37] Z. Arham, K. Kurniawan, and L. Anhusadar, Mater. Sci. Semicond. Process 106 (2023) 107466.
[38] Z. Arham, A.K. Ramli, M. Nurdin, and M. Natsir, Anal. Bioanal. Electrochem. 15 (2023) 711.
[39] J. Ghodsi, and A.A. Rafati, Electroanal. Chem. 807 (2017) 1.
[40] M. Daizy, M.R. Ali, M.S. Bacchu, M.A.S. Aly, and M.Z.H. Khan, Environ. Technol. Innov. 24 (2021) 101847.
[41] L. Killedar, D. Ilager, S.J. Malode, and N.P. Shetti, Mater. Chem. Phys. 285 (2022) 126131.
[42] A.M. Pai, M.M. Shanbhag, T. Maiyalagan, S.A. Alqarni, and N.P. Shetti, Diam. Relat. Mater. 140 (2023) 110561.